

# Realization of Arbitrary Gates in Holonomic Quantum Computation

Antti O. Niskanen, Mikio Nakahara,\* and Martti M. Salomaa  
*Materials Physics Laboratory, POB 2200 (Technical Physics),  
FIN-02015 HUT, Helsinki University of Technology, Finland*

Among the many proposals for the realization of a quantum computer, holonomic quantum computation (HQC) is distinguished from the rest in that it is geometrical in nature and thus expected to be robust against decoherence. Here we analyze the realization of various quantum gates by solving the inverse problem: Given a unitary matrix, we develop a formalism by which we find loops in the parameter space generating this matrix as a holonomy. We demonstrate for the first time that such a one-qubit gate as the Hadamard gate and such two-qubit gates as the CNOT gate, the SWAP gate and the discrete Fourier transformation can be obtained with a single loop.

PACS numbers: 03.65.Vf, 03.67.Lx, 02.60.Pn

Keywords: quantum computation, holonomy, complex projective space, numerical optimization

## I. INTRODUCTION

Quantum computing is an emerging scientific discipline, in which the merging and mutual cross-fertilization of two of the most important developments in physical science and information technology of the past century — quantum mechanics and computing — has resulted in an extraordinarily rapid rate of progress of interdisciplinary nature. Interesting problems to address in this context include fundamental questions as to what are the ultimate physical limits of computation and communication. For introductions to quantum computing and quantum information processing see, e.g., Refs. [1, 2, 3].

Holonomic quantum computation (HQC) was first suggested by Zanardi and Rasetti in Ref. [4]. The concept has been further developed in Refs. [5, 6, 7, 8, 9]. The suggestion is very intriguing itself; quantum-logical operations are achieved by driving a degenerate system around adiabatic loops in the parameter manifold. The resulting gates are a generalization of the celebrated Berry phase [10] to encompass a degenerate system. These are, in fact, non-Abelian holonomies. Due to the geometric nature of these gates, quantum information processing is expected to be fault tolerant. For instance the issue of timing and the lack of spontaneous decay are definite strengths of HQC. Here we study the construction of holonomic quantum-logic gates numerically for the first time via solving a certain inverse problem. Namely, we find the loop  $\hat{\gamma}$  corresponding to the desired unitary operator  $\hat{U}$  by solving a high-dimensional optimization task.

The paper is organized as follows: In Section II, we present the physical and mathematical background underlying our approach. Sections III, IV and V comprise the main part of the present paper. Loop parameterizations for one- and two-qubit gates are presented in Section III. The numerical method is introduced in Sec-

tion IV. Then the optimal realization of a unitary gate as a holonomy associated with a loop in the parameter space is investigated numerically in Section V. Section VI discusses the results.

## II. HAMILTONIAN AND HOLONOMY

Here we first review the concept of non-Abelian holonomy to establish notation conventions. Let us consider a family of Hamiltonians  $\{H_\lambda\}$ . The point  $\lambda$ , continuously parameterizing the Hamiltonian, is an element of a manifold  $\mathcal{M}$  called the control manifold and the local coordinate of  $\lambda$  is denoted by  $\lambda^i$  ( $1 \leq i \leq m = \dim \mathcal{M}$ ). It is assumed that there exists only a finite number of eigenvalues  $\varepsilon_k(\lambda)$  ( $1 \leq k \leq R$ ) for an arbitrary  $\lambda \in \mathcal{M}$  and that no level crossings occur. Suppose the  $n$ -th eigenvalue  $\varepsilon_n(\lambda)$  is  $g_n$ -fold degenerate for any  $\lambda \in \mathcal{M}$  and  $\sum_{n=1}^R g_n = N$ . The degenerate subspace at  $\lambda$  is denoted by  $\mathcal{H}_n(\lambda)$ . Accordingly, the Hamiltonian is expressed as an  $N \times N$  matrix. The orthonormal basis vectors of  $\mathcal{H}_n(\lambda)$  are denoted by  $\{|n\alpha; \lambda\rangle\}$ ;

$$H_\lambda |n\alpha; \lambda\rangle = \varepsilon_n(\lambda) |n\alpha; \lambda\rangle, \quad \langle n\alpha; \lambda | m\beta; \lambda \rangle = \delta_{mn} \delta_{\alpha\beta}.$$

Note that there are  $U(g_n)$  degrees of freedom in the choice of the basis vectors  $\{|n\alpha; \lambda\rangle\}$ .

Let us now assume that the parameter  $\lambda$  is changed adiabatically. We will be concerned with a particular subspace, say the ground state  $\mathcal{H}_1(\lambda)$  and we drop the index  $n$  to simplify the notation. Suppose the initial state at  $t = 0$  is an eigenstate  $|\psi_\alpha(0)\rangle = |\alpha; \lambda(0)\rangle$  with the energy  $\varepsilon = 0$  possibly through shifting the zero-point of the energy. In fact, we are not interested in the dynamical phase at all and hence assume that the eigenvalue in this subspace vanishes for any  $\lambda \in \mathcal{M}$ . The Schrödinger equation is

$$i \frac{d}{dt} |\psi_\alpha(t)\rangle = H_{\lambda(t)} |\psi_\alpha(t)\rangle, \quad (1)$$

\*Also at Department of Physics, Kinki University, Higashi-Osaka 577-8502, Japan.

whose solution may be assumed to take the form

$$|\psi_\alpha(t)\rangle = \sum_{\beta=1}^g |\beta; \lambda(t)\rangle U_{\beta\alpha}(t). \quad (2)$$

The unitarity of the matrix  $U_{\beta\alpha}(t)$  follows from the normalization of  $|\psi_\alpha(t)\rangle$ . By substituting Eq. (2) into (1), one finds that  $U_{\beta\alpha}$  satisfies

$$\dot{U}_{\beta\alpha}(t) = - \sum_{\gamma} \left\langle \beta; \lambda(t) \left| \frac{d}{dt} \right| \gamma; \lambda(t) \right\rangle U_{\gamma\alpha}. \quad (3)$$

The formal solution may be expressed as

$$\begin{aligned} U(t) &= \mathcal{T} \exp \left( - \int_0^t A(\tau) d\tau \right) \\ &= I - \int_0^t A(\tau) d\tau \\ &\quad + \int_0^t d\tau \int_0^\tau d\tau' A(\tau) A(\tau') + \dots, \end{aligned} \quad (4)$$

where  $\mathcal{T}$  is the time-ordering operator and

$$A_{\beta\alpha}(t) = \left\langle \beta; \lambda(t) \left| \frac{d}{dt} \right| \alpha; \lambda(t) \right\rangle.$$

Let us introduce the Lie-algebra-valued connection

$$\mathcal{A}_{i,\beta\alpha} = \left\langle \beta; \lambda(t) \left| \frac{\partial}{\partial \lambda^i} \right| \alpha; \lambda(t) \right\rangle \quad (5)$$

through which  $U(t)$  is expressed as

$$U(t) = \mathcal{P} \exp \left( - \int_{\lambda(0)}^{\lambda(t)} \mathcal{A}_i d\lambda^i \right), \quad (6)$$

where  $\mathcal{P}$  is the path-ordering operator. Note that  $\mathcal{A}_i$  is anti-Hermitian,  $\mathcal{A}_i^\dagger = -\mathcal{A}_i$ .

Suppose the path  $\lambda(t)$  is a loop  $\gamma(t)$  in  $\mathcal{M}$  such that  $\gamma(0) = \gamma(T) = \lambda_0$ . Then it is found after traversing  $\gamma$  that one ends up with the state

$$|\psi_\alpha(T)\rangle = \sum_{\beta=1}^g |\psi_\beta(0)\rangle U_{\beta\alpha}(T) \quad (7)$$

where use has been made of the definition  $|\psi_\beta(0)\rangle = |\beta; \lambda_0\rangle$ . The unitary matrix

$$U_\gamma \equiv U(T) = \mathcal{P} \exp \left( - \oint_\gamma \mathcal{A}_i d\gamma^i \right) \quad (8)$$

is called the holonomy associated with the loop  $\gamma(t)$ . Note that  $U_\gamma$  is independent of the parameterization of the path but only depends upon its geometric image in  $\mathcal{M}$ .

The space of all the loops based at  $\lambda_0$  is denoted

$$L_{\lambda_0}(\mathcal{M}) = \{\gamma : [0, T] \rightarrow \mathcal{M} | \gamma(0) = \gamma(T) = \lambda_0\}. \quad (9)$$

The set of the holonomy

$$\text{Hol}(\mathcal{A}) = \{U_\gamma | \gamma \in L_{\lambda_0}(\mathcal{M})\} \quad (10)$$

has a group structure [13] and is called the holonomy group. It is clear that  $\text{Hol}(\mathcal{A}) \subset U(g)$ . The connection  $\mathcal{A}$  is called irreducible when  $\text{Hol}(\mathcal{A}) = U(g)$ .

### III. THREE-STATE MODEL AND QUANTUM-GATE CONSTRUCTION

#### A. One-qubit gates

To make things tractable, we employ a simple model Hamiltonian called the three-state model as the basic building block for our strategy. This is a 3-dimensional Hamiltonian with the matrix form

$$H_{\lambda_0} = \epsilon |2\rangle\langle 2| = \begin{pmatrix} \epsilon & 0 & 0 \\ 0 & 0 & 0 \\ 0 & 0 & 0 \end{pmatrix}. \quad (11)$$

The first column (row) of the matrix refers to the auxiliary state  $|2\rangle$  with the energy  $\epsilon > 0$  while the second and the third columns (rows) refer to the vectors  $|0\rangle$  and  $|1\rangle$ , respectively, with vanishing energy. The qubit consists of the last two vectors.

The control manifold of the Hamiltonian (11) is the complex projective space  $\mathbb{C}P^2$ . This is seen most directly as follows: The most general form of the isospectral deformation of the Hamiltonian is of the form  $H_\gamma \equiv W_\gamma H_{\lambda_0} W_\gamma^\dagger$ , where  $W_\gamma \in U(3)$ . Note, however, that not all the elements of  $U(3)$  are independent. It is clear that  $H_\gamma$  is independent of the overall phase of  $W_\gamma$ , which reduces the number of degrees of freedom from  $U(3)$  to  $U(3)/U(1) = SU(3)$ . Moreover, any element of  $SU(3)$  may be decomposed into a product of three  $SU(2)$  matrices as follows

$$W_\gamma = \underbrace{\begin{pmatrix} \bar{\beta}_1 & \bar{\alpha}_1 & 0 \\ -\alpha_1 & \beta_1 & 0 \\ 0 & 0 & 1 \end{pmatrix}}_{U_1} \underbrace{\begin{pmatrix} \bar{\beta}_2 & 0 & \bar{\alpha}_2 \\ 0 & 1 & 0 \\ -\alpha_2 & 0 & \beta_2 \end{pmatrix}}_{U_2} \underbrace{\begin{pmatrix} 1 & 0 & 0 \\ 0 & \bar{\beta}_3 & \bar{\alpha}_3 \\ 0 & -\alpha_3 & \beta_3 \end{pmatrix}}_{U_3}, \quad (12)$$

which is known as the Givens decomposition. Here  $\alpha_j = e^{i\phi_j} \sin \theta_j$  and  $\beta_j = e^{i\psi_j} \cos \theta_j$ . It is clear that  $H_\gamma$  is independent of  $U_3$  since  $[H_{\lambda_0}, U_3] = 0$ . This further reduces the physical degrees of freedom to  $SU(3)/SU(2) \cong S^5$ . The product  $U_1 U_2$  contains six parameters while  $S^5$  is five-dimensional; there must be one redundant parameter in  $U_1 U_2$ . This parameter is easily found out by writing the product explicitly. The result depends only on the combination  $\phi_2 - \psi_2$  and not on individual parameters. Accordingly, we may redefine  $\phi_2$  as  $\phi_2 - \psi_2$  to eliminate  $\psi_2$ . Furthermore, after this redefinition we find that the Hamiltonian depends only on  $\phi_1 - \psi_1$  and  $\phi_2 - \psi_1$  and hence  $\psi_1$  may also be subsumed by redefining  $\phi_1$  and  $\phi_2$ ,

which reduces the independent degrees of freedom down to  $\mathbb{C}P^2 \cong S^5/S^1$ .

Let  $[z^1, z^2, z^3]$  be the homogeneous coordinate of  $\mathbb{C}P^2$  and  $(1, \xi_1, \xi_2)$  be the corresponding inhomogeneous coordinate, where  $\xi_1 = z^2/z^1, \xi_2 = z^3/z^1$  in the coordinate neighborhood with  $z^1 \neq 0$ . If we write  $\xi_k = r_k e^{i\varphi_k}$ , the above correspondence, i.e. the embedding of  $\mathbb{C}P^2$  into  $U(3)$ , is explicitly given by  $\theta_k = \tan^{-1} r_k$  and  $\phi_k = \varphi_k$ .

The connection coefficients are easily calculated in the present model and are given by

$$\mathcal{A}_{\theta_1} = \begin{pmatrix} 0 & -\sin \theta_2 e^{-i(\phi_2 - \phi_1)} \\ \sin \theta_2 e^{i(\phi_2 - \phi_1)} & 0 \end{pmatrix}, \quad (13)$$

$$\mathcal{A}_{\theta_2} = \begin{pmatrix} 0 & 0 \\ 0 & 0 \end{pmatrix}, \quad (14)$$

$$\mathcal{A}_{\phi_1} = \begin{pmatrix} -i \sin^2 \theta_1 & -\frac{i}{2} \sin 2\theta_1 \sin \theta_2 e^{i(\phi_1 - \phi_2)} \\ -\frac{i}{2} \sin 2\theta_1 \sin \theta_2 e^{i(\phi_2 - \phi_1)} & i \sin^2 \theta_2 \sin^2 \theta_1 \end{pmatrix}, \quad (15)$$

$$\mathcal{A}_{\phi_2} = \begin{pmatrix} 0 & 0 \\ 0 & -i \sin^2 \theta_2 \end{pmatrix}, \quad (16)$$

where the first column (row) refers to  $|0\rangle$  while the second one refers to  $|1\rangle$ . Using these connection coefficients, it is possible to evaluate the holonomy associated with a loop  $\gamma$  as

$$U_\gamma = \mathcal{P} \exp \left( - \oint_\gamma (\mathcal{A}_{\theta_1} d\theta_1 + \mathcal{A}_{\theta_2} d\theta_2 + \mathcal{A}_{\phi_1} d\phi_1 + \mathcal{A}_{\phi_2} d\phi_2) \right). \quad (17)$$

Now our task is to find a loop that yields a given unitary matrix as its holonomy.

## B. Two-qubit gates

Let us consider a two-qubit reference Hamiltonian

$$H_{\lambda_0}^{2\text{-qubit}} = H_{\lambda_0}^a \otimes I_3 + I_3 \otimes H_{\lambda_0}^b, \quad (18)$$

where  $H_{\lambda_0}^{a,b}$  are three-state Hamiltonians and  $I_3$  is the  $3 \times 3$  unit matrix. Generalization to an arbitrary  $N$ -qubit system is obvious. The Hamiltonian scales as  $3^N$ , instead of the  $2^N$  in the present model. It is also possible to consider a model with  $g$ -degenerate eigenstates with one auxiliary state having finite energy. This model, however, has a difficulty in realizing an entangled state, without which the full computational power of a quantum computer is impossible.

We want to maintain the multipartite structure of the system in constructing the holonomy. For this purpose,

we separate the unitary transformation into a product of single-qubit transformations ( $W_\gamma^a \otimes W_\gamma^b$ ) and a purely two-qubit rotation  $W_\gamma^{2\text{-qubit}}$  which cannot be reduced into a tensor product of single-qubit transformations. Therefore, we write the iso-spectral deformation for a given loop  $\gamma$  as

$$H_\gamma^{2\text{-qubit}} = W_\gamma^{2\text{-qubit}} (W_\gamma^a \otimes W_\gamma^b) H_{\lambda_0}^{2\text{-qubit}} \times (W_\gamma^a \otimes W_\gamma^b)^\dagger W_\gamma^{2\text{-qubit}\dagger}. \quad (19)$$

The advantage of expressing the unitary matrix in this form is easily verified when we write down the connection coefficients for the one-qubit coordinates. Namely, the two-qubit transformation does not affect the one-qubit transformation at all;

$$\begin{aligned} \mathcal{A}_{i,\alpha\beta} &= \left\langle \alpha; \lambda \left| W_\gamma^\dagger \frac{\partial}{\partial \gamma^i} W_\gamma \right| \beta; \lambda \right\rangle \\ &= \left\langle \alpha; \lambda \left| (W_\gamma^a \otimes W_\gamma^b)^\dagger \frac{\partial}{\partial \gamma^i} (W_\gamma^a \otimes W_\gamma^b) \right| \beta; \lambda \right\rangle, \end{aligned}$$

where  $\gamma^i$  denotes a one-qubit coordinate.

There is a large number of possible choices for  $W_\gamma^{2\text{-qubit}}$ , depending on the physical realization of the present scenario. To keep our analysis as concrete as possible, we have made the simplest choice

$$W_\gamma^{2\text{-qubit}} = W_\xi \equiv e^{i\xi|11\rangle\langle 11|} \quad (20)$$

for our two-qubit unitary rotation. Let

$$\begin{aligned}
H'_\gamma &= H_\gamma^a \otimes I_3 + I_3 \otimes H_\gamma^b \\
&= \begin{pmatrix} h_{11}^a+h_{11}^b & h_{12}^b & h_{13}^b & h_{12}^a & 0 & 0 & h_{13}^a & 0 & 0 \\ h_{21}^b & h_{11}^a+h_{22}^b & h_{23}^b & 0 & h_{12}^a & 0 & 0 & h_{13}^a & 0 \\ h_{31}^b & h_{32}^b & h_{11}^a+h_{33}^b & 0 & 0 & h_{12}^a & 0 & 0 & h_{13}^b \\ h_{21}^a & 0 & 0 & h_{22}^a+h_{11}^b & h_{12}^b & h_{13}^b & h_{23}^a & 0 & 0 \\ 0 & h_{21}^a & 0 & h_{21}^b & h_{22}^a+h_{22}^b & h_{23}^b & 0 & h_{23}^a & 0 \\ 0 & 0 & h_{21}^a & h_{31}^b & h_{32}^b & h_{22}^a+h_{33}^b & 0 & 0 & h_{23}^b \\ h_{31}^a & 0 & 0 & h_{32}^a & 0 & 0 & h_{33}^a+h_{11}^b & h_{12}^b & h_{13}^b \\ 0 & h_{31}^a & 0 & 0 & h_{32}^a & 0 & h_{21}^b & h_{33}^a+h_{22}^b & h_{23}^b \\ 0 & 0 & h_{31}^a & 0 & 0 & h_{32}^a & h_{31}^b & h_{32}^b & h_{33}^a+h_{33}^b \end{pmatrix}.
\end{aligned}$$

be a two-qubit Hamiltonian before  $W_\xi$  is applied. Then after the application of  $W_\xi$  to  $H'_\gamma$  we have the full Hamiltonian

$$\begin{aligned}
H_\gamma^{2\text{-qubit}} &= W_\xi H'_\gamma W_\xi^\dagger \\
&= \begin{pmatrix} h_{11}^a+h_{11}^b & h_{12}^b & h_{13}^b & h_{12}^a & 0 & 0 & h_{13}^a & 0 & 0 \\ h_{21}^b & h_{11}^a+h_{22}^b & h_{23}^b & 0 & h_{12}^a & 0 & 0 & h_{13}^a & 0 \\ h_{31}^b & h_{32}^b & h_{11}^a+h_{33}^b & 0 & 0 & h_{12}^a & 0 & 0 & h_{13}^b e^{-i\xi} \\ h_{21}^a & 0 & 0 & h_{22}^a+h_{11}^b & h_{12}^b & h_{13}^b & h_{23}^a & 0 & 0 \\ 0 & h_{21}^a & 0 & h_{21}^b & h_{22}^a+h_{22}^b & h_{23}^b & 0 & h_{23}^a & 0 \\ 0 & 0 & h_{21}^a & h_{31}^b & h_{32}^b & h_{22}^a+h_{33}^b & 0 & 0 & h_{23}^b e^{-i\xi} \\ h_{31}^a & 0 & 0 & h_{32}^a & 0 & 0 & h_{33}^a+h_{11}^b & h_{12}^b & h_{13}^b e^{-i\xi} \\ 0 & h_{31}^a & 0 & 0 & h_{32}^a & 0 & h_{21}^b & h_{33}^a+h_{22}^b & h_{23}^b e^{-i\xi} \\ 0 & 0 & h_{31}^a e^{i\xi} & 0 & 0 & h_{32}^a e^{i\xi} & h_{31}^b e^{i\xi} & h_{32}^b e^{i\xi} & h_{33}^a+h_{33}^b \end{pmatrix}. \quad (21)
\end{aligned}$$

As for the connection, we find

$$\mathcal{A}_\xi = \begin{pmatrix} 0 & 0 & 0 & 0 \\ 0 & 0 & 0 & 0 \\ 0 & 0 & 0 & 0 \\ 0 & 0 & 0 & i \cos^2 \theta_2^a \cos^2 \theta_2^b \end{pmatrix} \quad (22)$$

where the columns and rows are ordered with respect to the basis  $\{|00\rangle, |01\rangle, |10\rangle, |11\rangle\}$ . It should be apparent from the above analysis that we can construct an arbitrary controlled phase-shift gate with the help of a loop in the  $(\theta_2^a, \xi)$ - or  $(\theta_2^b, \xi)$ -space. Accordingly, this gives the CNOT gate with one-qubit operations, as shown below.

### C. Some Examples

Before we proceed to present the numerical prescription to construct arbitrary one- and two-qubit gates in the next section, it is instructive to first work out some important examples whose loop can be constructed analytically. In particular, we will show that all the gates required for the proof of universality may be obtained within the present three-state model.

The first example is the  $\pi/8$ -gate,

$$U_{\pi/8} = \begin{pmatrix} 1 & 0 \\ 0 & e^{i\pi/8} \end{pmatrix}. \quad (23)$$

By inspecting the connection coefficients in Eqs. (13-16), we easily find that the loop presented by the sequence

$$\begin{aligned}
(\theta_2, \phi_2) &: (0, 0) \rightarrow (\pi/2, 0) \rightarrow (\pi/2, \pi/8) \\
&\rightarrow (0, \pi/8) \rightarrow (0, 0). \quad (24)
\end{aligned}$$

yields the desired gate. Note that the loop is in the  $(\theta_2, \phi_2)$ -plane and that all the other parameters are fixed at zero. Explicitly, we verify that

$$\begin{aligned}
U_{\pi/8} &= \exp\left(\frac{\pi}{8} \mathcal{A}_{\phi_2} |_{\theta_2=0}\right) \exp\left(\frac{\pi}{2} \mathcal{A}_{\theta_2} |_{\phi_2=\pi/8}\right) \\
&\quad \times \exp\left(-\frac{\pi}{8} \mathcal{A}_{\phi_2} |_{\theta_2=\pi/2}\right) \exp\left(-\frac{\pi}{2} \mathcal{A}_{\theta_2} |_{\phi_2=0}\right) \\
&= \exp\left(-\frac{\pi}{8} \mathcal{A}_{\phi_2} |_{\theta_2=\pi/2}\right). \quad (25)
\end{aligned}$$

The next example is the Hadamard gate

$$H = \frac{1}{\sqrt{2}} \begin{pmatrix} 1 & 1 \\ 1 & -1 \end{pmatrix}. \quad (26)$$

Instead of constructing  $H$  directly, we will rather use the decomposition

$$H = e^{-i\pi/2} \exp\left(i\frac{\pi}{2}\sigma_z\right) \exp\left(i\frac{\pi}{4}\sigma_y\right).$$

It is easy to verify that the holonomy associated with the loop

$$\begin{aligned}
(\theta_2, \theta_1) &: (0, 0) \rightarrow (\pi/2, 0) \rightarrow (\pi/2, \beta) \\
&\rightarrow (0, \beta) \rightarrow (0, 0) \quad (27)
\end{aligned}$$

is  $\exp(i\beta\sigma_y)$ , while that associated with the loop

$$\begin{aligned}
(\theta_1, \theta_2, \phi_1) &: (0, 0, 0) \rightarrow (\pi/2, 0, 0) \rightarrow (\pi/2, \pi/2, 0) \\
&\rightarrow (\pi/2, \pi/2, \alpha) \rightarrow (\pi/2, 0, \alpha) \\
&\rightarrow (0, 0, \alpha) \rightarrow (0, 0, 0) \quad (28)
\end{aligned}$$

is  $\exp(i\alpha\sigma_z)$ . Here again, the rest of the parameters are fixed at zero. Finally, we construct the phase-shift gate



FIG. 1: Objective function landscape in 2D.

$e^{i\delta}$ , which is produced by a sequence of two loops. First we construct a gate similar to the  $\delta$ -shift gate using (cf., the  $\pi/8$ -shift gate)

$$\begin{aligned} (\theta_1, \phi_1) : (0, 0) &\rightarrow (\pi/2, 0) \rightarrow (\pi/2, \delta) \\ &\rightarrow (0, \delta) \rightarrow (0, 0). \end{aligned} \quad (29)$$

This loop followed by the similar loop in the  $(\theta_2, \phi_2)$ -space yields the  $e^{i\delta}$ -gate as

$$\begin{aligned} (\theta_1, \phi_1, \theta_2, \phi_2) : \\ (0, 0, 0, 0) &\rightarrow (0, 0, \pi/2, 0) \rightarrow (0, 0, \pi/2, \delta) \\ &\rightarrow (0, 0, 0, \delta) \rightarrow (0, 0, 0, 0) \rightarrow (\pi/2, 0, 0, 0) \\ &\rightarrow (\pi/2, \delta, 0, 0) \rightarrow (0, \delta, 0, 0) \rightarrow (0, 0, 0, 0). \end{aligned} \quad (30)$$

Finally, the controlled-phase gate  $U(\Theta) = \exp(i\Theta|11\rangle\langle 11|)$  can be written as

$$\begin{aligned} (\theta_2^a, \xi) : (0, 0) &\rightarrow (\pi/2, 0) \rightarrow (\pi/2, \Theta) \\ &\rightarrow (0, \Theta) \rightarrow (0, 0). \end{aligned} \quad (31)$$

#### IV. NUMERICAL METHOD

Now we adopt a systematic approach to actually constructing arbitrary quantum gates. This is the first time that arbitrary one- and two-qubit gates are constructed in a three-state model that is in a way the simplest possible realization for HQC while still maintaining the tensor-product structure necessary for exponential speed-up. It has not been shown previously how to construct the CNOT, let alone the two-qubit Fourier transform in a single loop. Hence, we resort to numerical methods. Since it is extremely difficult to see which single loop results in a given unitary operator, our approach will be that of variational calculus.

We convert the inverse problem, i.e. which loop corresponds to a given unitary operator, to an optimization problem. The problem of finding the unitary operator for a given loop is straightforward. Keeping the basepoint

NODE	$\theta_1$	$\theta_2$	$\phi_1$	$\phi_2$
begin	0	0	0	0
1	-5.28	2.04	0.18	-0.40
2	-0.44	1.49	-0.08	3.70
3	-0.70	-0.27	-0.11	2.59
end	0	0	0	0

TABLE I: Loop of Fig. 2 numerically.

of the holonomy loop fixed, we let the midpoints vary. Owing to the  $2\pi$ -periodicity, the loops can end either in the origin or at any point that is modulo  $2\pi$ .

The space of all possible loops is denoted by  $\mathcal{V}$ . We shall restrict the variational task to the space of polygonal paths  $\mathcal{V}_k$ , where  $k$  is the number of vertices in the path excluding the basepoint. Naturally, we have  $\mathcal{V}_k \subset \mathcal{V}$  such that we are not guaranteed to find the best possible solution among all the loops, but provided that we use a good optimization method, we may expect to find the best solution in the limited space  $\mathcal{V}_k$ . Since the dimension of the variational space increases with  $k$ , one is forced to use as low a  $k$  as possible. For instance, for one-qubit gates the dimension is  $4k$ . In the case of two-qubit gates the dimension is  $9k$ . Low  $k$  appears to be desirable for experimental reasons as well.

Formally, the optimization problem is to find a  $\tilde{\gamma}$ , such that

$$f(\gamma) = \|\hat{U} - U_\gamma\|_F \quad (32)$$

is minimized over all  $\gamma \in \mathcal{V}_k$ . We naturally hope the minimum value to be zero. Here  $\|\cdot\|_F$  is the so-called Frobenius trace norm defined by  $\|A\|_F = \sqrt{\text{Tr}(A^\dagger A)}$ . We could employ the well-known conjugate-gradient method to solve the task at hand but this method, or any other derivative-based method, is not expected to perform well in the present problem due to the complicated structure of the objective function. Hence we will use the robust polytope algorithm [14].

We have plotted a sample 2D section of the optimization space in Fig. 1. The axes represent two orthogonal directions in the optimization space of a certain two-qubit gate. The  $x$ -axis was obtained by interpolating between two known minima, whereas the  $y$ -axis was chosen randomly. One can readily verify from the figure that the optimization task is indeed extremely hard.

The calculation of the holonomy requires evaluating the ordered product in Eq. (8). The method used in the numerical algorithm is to simply write the ordered product in a finite-difference approximation by considering the connection components as being constant over a small difference in the parameters  $\delta\gamma_i$ , i.e.

$$U_\gamma \approx \exp(-\mathcal{A}_i(\gamma_n)\delta\gamma_n^i) \cdots \exp(-\mathcal{A}_i(\gamma_1)\delta\gamma_1^i). \quad (33)$$

Throughout the study we used 200 discretization points per edge, i.e.,  $n = 200 \times (k + 1)$ .

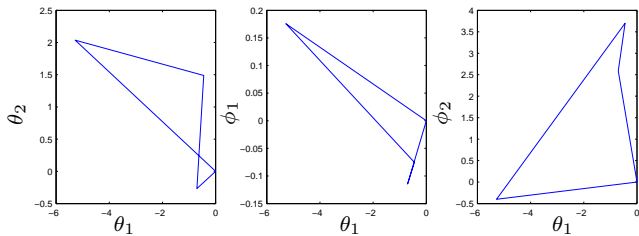


FIG. 2: Loop in parameter space that gives the Hadamard gate.

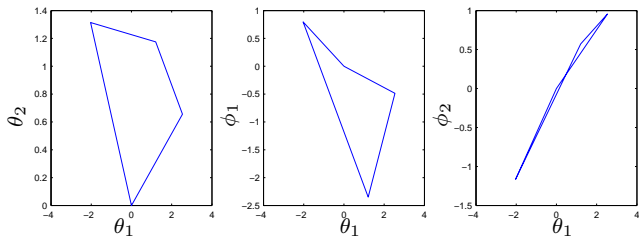


FIG. 3: Loop in parameter space that yields the gate  $U = e^i \exp(i\frac{\pi}{7}\sigma_z) \exp(i\frac{1}{3}\sigma_y) \exp i\sigma_z$ .

## V. RESULTS

First we attempted to find a loop that yields the Hadamard gate. Using a random initial configuration, we obtained the results that are plotted in Fig. 2. The error function  $f(\gamma)$  had a value smaller than  $10^{-8}$  at the numerical optimum. The plot represents all the possible projections on two perpendicular axes (the horizontal axis is always  $\theta_1$ ) in the four-dimensional space. Note that this optimization was carried out in  $\mathcal{V}_3$ , meaning that there are three vertices other than the reference point. The results do not take advantage of the  $2\pi$  periodicity. We have also included the data points in Table I. It is impressive that such a simple control loop yields the gate. Furthermore, this is just one implementation of the Hadamard gate. It is possible to find many different ones.

Another example of one-qubit gates is given in Fig. 3 and in Table II. The gate that we tried to implement was now chosen arbitrarily to be  $U = e^i \exp(i\frac{\pi}{7}\sigma_z) \exp(i\frac{1}{3}\sigma_y) \exp i\sigma_z$ . Again, the error was well below  $10^{-8}$  at the optimum. We argue that our method is capable of finding any one-qubit gate. These

NODE	$\theta_1$	$\theta_2$	$\phi_1$	$\phi_2$
begin	0	0	0	0
1	-2.03	1.31	0.80	-1.16
2	1.21	1.18	-2.35	0.57
3	2.54	0.66	-0.49	0.96
end	0	0	0	0

TABLE II: Loop of Fig. 3 numerically.

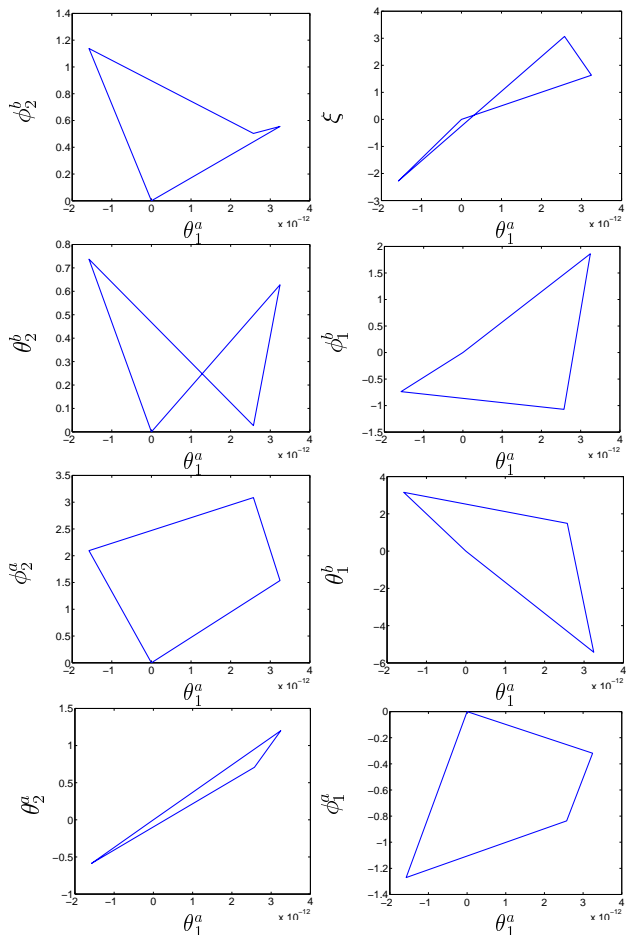


FIG. 4: Loop in parameter space that gives the CNOT gate. Here  $\gamma_{\text{CNOT}} \in \mathcal{V}_3$  and the error is below  $10^{-13}$ .

results are not very enlightening as such, but should nevertheless clearly prove the strength of the technique.

We also found several implementations for two-qubit gates. Figure 4 presents the loop  $\gamma_{\text{CNOT}} \in \mathcal{V}_3$  that produces the CNOT. We observe, however, that again the minimization resulted in an accurate solution. The minimization landscape is just as rough in the case of two qubits. Now, of course, the dimension of  $\mathcal{V}_3$  is 24.

We also found an implementation of the SWAP gate given in Fig. 5.

Finally, it is interesting to observe that even the two-qubit quantum Fourier transform can be performed easily. The resulting loop is presented in Fig. 6. It is remarkable that such a simple single loop yields a two-qubit quantum Fourier transform. We used only three vertices but were still able to find an acceptable solution. We argue that the error can be made arbitrarily small for any two-qubit gate.

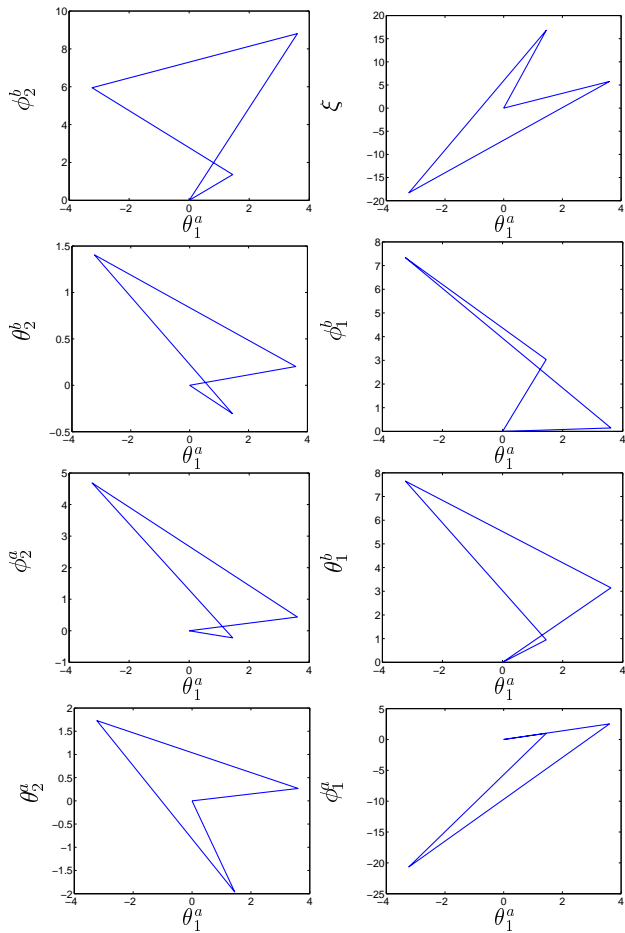


FIG. 5: Loop in parameter space which realizes the SWAP gate. Here the error is below  $10^{-13}$ . In this case the variational space is  $\mathcal{V}_5$ .

## VI. DISCUSSION

The realization of arbitrary one- and two-qubit gates in the context of holonomic quantum computation has been demonstrated. By restricting the loops in the control manifold within a polygon with  $k$  vertices, it becomes possible to cast the realization problem to a finite-dimensional variational problem. We have shown explicitly that some useful two-qubit gates are realized by a single loop.

A possible improvement of the present scenario would be to minimize the length of the path realizing a given gate. This can be carried out by introducing an appropriate penalty or barrier function and the Fubini-Study metric in the control manifold  $CP^2$ . This optimization

program is under progress and will be reported elsewhere.

## Acknowledgments

AN would like to thank the Research Foundation of Helsinki University of Technology and the Gradu-

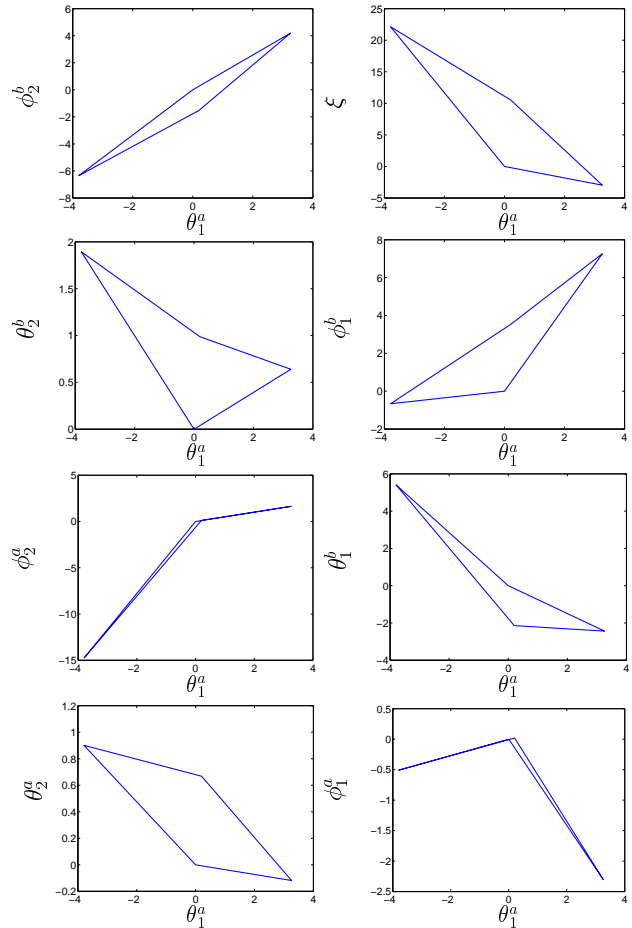


FIG. 6: Loop  $\gamma_{\text{Fourier}}$ . The error is below  $10^{-13}$ .

ate School in Technical Physics for financial support; MN thanks the Helsinki University of Technology for a Visiting Professorship and he is also grateful for partial support of Grant-in-Aid from the Ministry of Education, Science, Sports and Culture, Japan (Project Nos. 14540346 and 13135215); MMS acknowledges the Academy of Finland for a Research Grant in Theoretical Materials Physics.

- 
- [1] J. Gruska, *Quantum Computing*, McGraw-Hill, New York (1999).  
 [2] M. A. Nielsen and I.L. Chuang, *Quantum Computation and Quantum Information*, Cambridge University Press,

- Cambridge (2000).  
 [3] A. Galindo and M. A. Martin-Delgado, *Rev. Mod. Phys.* **74**, 347(2002).  
 [4] P. Zanardi and M. Rasetti, *Phys. Lett. A.* **264**, 94 (1999).

- [5] K. Fujii, Rep. Math. Phys. **48**, 75 (2001).
- [6] D. Ellinas and J. Pachos, Phys. Rev. A. **64**, 022310 (2001).
- [7] J. Pachos, P. Zanardi and M. Rasetti, Phys. Rev. A. **61**, 010305(R) (1999).
- [8] J. Pachos, P. Zanardi, Int. J. Mod. Phys **15**, 1257 (2001).
- [9] J. Pachos and S. Chountasis, Phys. Rev. A. **62**, 052318 (2000).
- [10] M. Berry, Proc. R. Soc. Lond. A **392**, 45 (1984).
- [11] A. Zee, Phys. Rev. A **38**, 1 (1988).
- [12] F. Wilczek and A. Zee, Phys. Rev. Lett. **52**, 2111 (1984).
- [13] M. Nakahara, *Geometry, Topology and Physics*, IOP Publishing Ltd., Bristol (1990).
- [14] J. C. Lagarias, J. A. Reeds, M. H. Wright, and P. E. Wright, *Convergence Properties of the Nelder-Mead Simplex Method in Low Dimensions*, SIAM Journal of Optimization **9**, 112 (1998).